





[View Journal Online](#)  
[View Article Online](#)

# Biogenic synthesis of selenium nanoparticles using *Hibiscus esculentus* L. extract: Catalytic degradation of organic dye and its anticancer, antibacterial and antifungal activities

Mohammad Ali Ebrahimzadeh , Mina Moradsomarein ,  
 Fatemeh Sadeghi Lalerdi  and Seyedeh Roya Alizadeh \*

Department of Medicinal Chemistry, School of Pharmacy and Pharmaceutical Sciences Research Center, Mazandaran University of Medical Sciences, Sari, 4815733971, Iran

\* Corresponding author at: Department of Medicinal Chemistry, School of Pharmacy and Pharmaceutical Sciences Research Center, Mazandaran University of Medical Sciences, Sari, 4815733971, Iran.

e-mail: [r.alizadeh.2019@gmail.com](mailto:r.alizadeh.2019@gmail.com) (S.R. Alizadeh).

## RESEARCH ARTICLE

## ABSTRACT



doi 10.5155/eurjchem.14.1.144-154.2401

Received: 24 December 2022

Received in revised form: 21 January 2023

Accepted: 28 January 2023

Published online: 31 March 2023

Printed: 31 March 2023

## KEYWORDS

Catalytic effect  
 Methylene blue  
 Green synthesis  
 Anticancer activity  
 Antibacterial activity  
 Selenium nanoparticles

In this work, we develop the synthesis of selenium nanoparticles (B@SeNPs) using a green method using the aqueous extract of *Hibiscus esculentus* L. Various techniques were used to characterize bio-synthesized B@SeNPs. The mixture color was clearly changed to reddish at 45-50 °C and the extract pH = 6. According to Fourier transform infrared spectroscopy (FT-IR), the B@SeNPs were produced, capped, and stabilized using biomolecules found in plant extracts. The energy dispersive X-ray (EDX) analysis profile revealed an atomic Se signal (1.39 mV). The powder X-ray diffraction (PXRD) pattern confirmed the hexagonal phase crystalline form of B@SeNPs. The zeta potential for SeNPs was determined to be -51.3 mV. Scanning electron microscope (SEM) and transmission electron microscopy (TEM) micrographs revealed spherical Se particles with sizes of roughly 62 nm. Furthermore, B@SeNPs can degrade methylene blue dye by 98.3% at 21 min with a rate constant of 0.1023 min<sup>-1</sup> in the presence of NaBH<sub>4</sub>. In biological evaluation, the synthesized nanoparticles have been proven to be effective against two human cancers (AGS and MCF-7 cells) with IC<sub>50</sub> values of 20.46 and 88.43 µg/mL, respectively. Additionally, B@SeNPs showed high safety in the Beas cell line (normal) at 123 µg/mL as the highest concentration. The biofabricated SeNPs had a moderate antibacterial effect against ATCC and multidrug-resistant clinical isolates. They had no antifungal activity against the tested fungus strains except *C. albicans* (IFRC 1873), with a MIC value of 138.75 µg/mL. Finally, the green-synthesized B@SeNPs could be a contender for further testing as a chemotherapeutic agent in the treatment of some human cancers.

Cite this: *Eur. J. Chem.* 2023, 14(1), 144-154

Journal website: [www.eurjchem.com](http://www.eurjchem.com)

## 1. Introduction

The dyeing and textile industries are to blame for water contamination. The removal of organic contaminants from industrial wastewater is critical for environmental technology [1,2]. Methylene blue (MB), a heterocyclic aromatic dye, is commonly used to colour cotton, wool, and silk in the textile industry. It reduces the amount of dissolved oxygen in water and releases toxic substances as a result of chemical or biological interactions, putting aquatic life in danger [3]. Various approaches can be used to degrade organic dye pollution. However, the expensive expense of some of these techniques, as well as their inability to remove soluble dyes and the use of chemicals, limit them. Of all dye removal techniques available, adsorption is one of the most efficient and affordable. Activated carbon is an effective adsorbent to separate dyes from industrial wastewater effluents, but its high cost prevents it from being used on a large scale [4]. In addition, photocatalysis is a method for purifying water that employs light to produce active species on light-sensitive molecules. Photocatalysis also has the

advantage of being low cost to operate and can work in any environment. Furthermore, degradation products are generally nontoxic and environmentally beneficial [1]. Throughout the past decade, nanotechnology has resulted in the discovery of materials with improved physicochemical features and applications ranging from nanoelectronics to nanomedicine [5]. Metallic and semiconductor nanoparticles are efficient dye degradation catalysts and photocatalysts in the aquatic environment [6-10].

Selenium nanoparticles (SeNPs) could be employed in a variety of applications. Selenium is a trace element that is vital for the nutritional and growth of the human body [11]. Therefore, as a result, they have received a great deal of attention in recent years and many synthetic methods have been used. A green method with plant extracts that requires nontoxic solvents and mild temperatures has gained favour as a cost-effective, environmentally friendly, and safe approach. Furthermore, it employs a biodegradable and readily available reducing agent [12,13]. Due to the high surface-to-volume ratio of selenium nanoparticles produced using plant extracts, they



Figure 1. The picture of *Hibiscus esculentus* L.

are also particularly effective materials for photocatalytic dye degradation [3,14]. SeNPs synthesized by leaf extract of *Fiscus benghalensis* degrade methylene blue dye at around 60% in 40 min [3]. In another study, bromothymol blue dye was removed using biogenic SeNP under UV illumination after 60 min at 62.3% [15]. Furthermore, biofabricated selenium nanoparticles demonstrated antibacterial, anti-diabetic, and cytotoxic properties [16]. In various studies, SeNPs have been shown to be effective against a variety of cancer cell lines [17-21], justifying the investigation of various physical, chemical, and biological manufacturing pathways. SeNPs are increasingly important in biomedical applications due to their anticancer characteristics. The action of colloidal SeNPs in human breast cancer cells was also established [1]. In this work, selenium nanoparticles are synthesized using an aqueous extract of *Abelmoschus esculentus* L.

Okra (*Hibiscus esculentus* L.) is known as a common vegetable in Bangladesh and the Indo-Pak subcontinent. It belongs to the Malvaceae family. It is the most consumed food in India, but originated in Ethiopia and Sudan. Furthermore, it is one of the oldest agricultural crops in the world, growing in numerous countries from Africa to Asia, southern Europe, and America [22]. In addition, it is named "bamyé" in Persian [22]. Although it is grown throughout the year, most of its production occurs during summer [23]. This fruit contains 86.1% water, 2.2 % protein, 0.2% fat, 9.7% carbohydrate, 1.0% fiber, and 0.8% ash [24], and also calcium, potassium, vitamins and other minerals are bound in this fruit. High levels of phenols and flavonoids were present in the extract [25]. In addition, efficient antihemolytic, antioxidant [25], and antihypoxic [22] activities of *H. esculentus* were confirmed.

In this study, the production of selenium nanoparticles using *Hibiscus esculentus* L. extract was described. Our research team has already demonstrated that *H. esculentus* extract is a valuable source for the fabrication of biogenic nanomaterials. The synthesized nanoparticles were characterized using various analytical methods. The anticancer, antibacterial, and antifungal activities of the synthesized SeNPs were investigated and used for photocatalytic degradation of MB under visible light and NaBH<sub>4</sub>.

## 2. Experimental

Sodium selenite and sodium borohydride were provided by Sigma Aldrich (USA) and Merck (Germany). Methylene blue and other chemicals were bought from Merck India Ltd.

### 2.1. Synthesis of selenium nanoparticles

The *H. esculentus* plant (Figure 1) was dried in the sun and cut into small sizes (2-3 mm). The plant (10 g) was added to 100 mL of deionized water, heated for 1 h at 50 °C, sonicated for 30 min, and filtrated by Whatman filter paper (No 1). The filtrate was used to synthesize SeNPs. 10 mL of aqueous extract was added to the stock solution Na<sub>2</sub>SeO<sub>3</sub> (0.01 M) at 45-50 °C and 500 rpm. After two days, the reaction color shifted from colorless to reddish, indicating that the Se ions had been reduced. After that, the solution containing SeNPs was washed four times with water and methanol, centrifuged, and dried in

an oven at 60 °C. The dried product was used for subsequent analyses.

### 2.2. Characterization of the synthesized SeNPs

The validation of prepared B@SeNPs was performed using UV-Vis spectrophotometer, T80 UV-Vis spectrophotometer PGI (Beijing, China) to evaluate the Surface Plasmon Resonance (SPR). The size and morphology of B@SeNPs were estimated by TEM Philips EM 208S and SEM TESCAN BRNO-Mira3 LMU. In addition, the EDX identified the purity and elemental composition of the fabricated B@SeNPs that was carried out along with SEM analysis. Next, the DLS study evaluated their average size dispersion. Following that, the crystallinity of SeNPs was determined by XRD analysis using PANalytical X-PERT PRO diffractometer ( $2\theta = 10-80^\circ$ ) with CuK $\alpha$  source ( $\lambda = 1.5406 \text{ \AA}$ ). To approve the capped SeNPs, the FT-IR analysis was applied to determine the potential molecules involved in the reduction of selenium ions (ATR, Agilent, Cary 630, FT-IR Spectrometer, equipment in 4000 and 650 cm<sup>-1</sup>).

### 2.3. Antibacterial activity of synthesised SeNPs

The antibacterial activity of bioproduced SeNPs using *H. esculentus* extract was tested against bacteria from the American Type Culture Collection (ATCC), comprising: *Proteus mirabilis*, *Klebsiella pneumoniae*, *Pseudomonas aeruginosa*, *Escherichia coli*, *Enterococcus faecalis*, *Staphylococcus aureus*, and *Acinetobacter baumannii*. In addition, the synthesized SeNPs were examined against eight multidrug resistant (MDR) bacteria isolated from clinical including: *P. mirabilis*, *K. pneumoniae*, *P. aeruginosa*, *E. coli*, *E. faecalis*, *S. aureus* (two strains), and *A. baumannii*. The minimum inhibitory concentration (MIC) of biosynthesized SeNPs was assessed using the microdilution method. In this experiment, positive control (conventional antibiotic ciprofloxacin) and negative control (medium and SeNPs) were used. One hundred microliters of Mueller-Hinton broth (MHB) with different amounts of SeNPs (277.5-0.27) were loaded into all wells. Subsequently, each well was filled with 100  $\mu$ L of dilute bacterial suspension (0.5 McFarland turbidity standards) and the plate was incubated at 37 °C. After that, the growth of bacteria in the wells was visually checked and the lowest concentration of SeNPs, which prevented the visible growth of bacteria in MHB, was determined as MIC. The minimum bactericidal concentration (MBC) was measured using Muller-Hinton agar media (MHA) on different plates according to the MIC value; 10  $\mu$ L from MIC well and three concentrated wells were cultured in MHA for 24 h at 37 °C. After 24 h, the MBC value was calculated as the lowest concentration of SeNPs that did not show observable growth in MHA [26-29].

### 2.4. Antifungal activity of synthesized SeNPs

Based on the M27-A3 method from the Clinical and Laboratory Standards Institute (CLSI), formerly NCCLS, the broth microdilution method was used to estimate the MIC value.

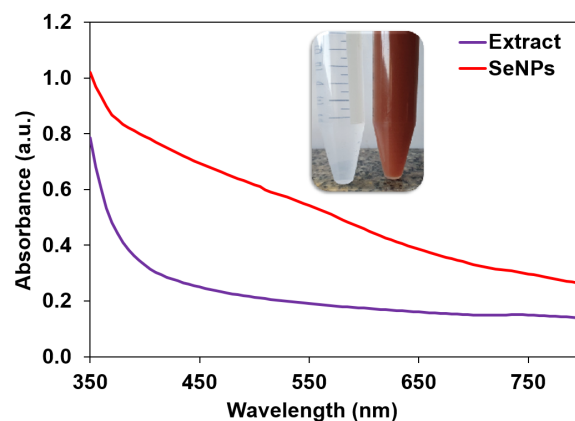


Figure 2. UV-vis spectra of B@SeNPs and *H. esculentus* L.

The tested strains contained *Candida albicans* (IFRC 1873), *Candida albicans* (IFRC 1874), *Aspergillus fumigatus* (IFRC 1649), *Aspergillus fumigatus* (IFRC 1505), *Trichophyton mentagrophytes* (FR1 22130), *Trichophyton mentagrophytes* (FR5 22130), *Fusarium proliferatum* (IFRC 1871), *Fusarium equiseti* (IFRC 1872). In summary, 100  $\mu\text{L}$  of B@SeNPs (555-0.54  $\mu\text{g}/\text{mL}$ ) were added to the microplate wells and serially diluted with 100  $\mu\text{L}$  of RPMI media. Then 100  $\mu\text{L}$  of cell suspensions were introduced into each well. Visible growth was checked after 24 h (*C. albicans*) and 48 h (other strains) under incubation conditions. Itraconazole was considered a reference antifungal agent [30,31].

### 2.5. Anticancer activity of synthesized SeNPs

The protocols mentioned earlier were used to determine cytotoxicity [32]. From the pasture Institute in Iran, human gastric cancer (AGS), human breast adenocarcinoma (MCF-7), and human non-tumorigenic lung epithelial cell line (Beas) cells were generated. The dimethyl thiazolyl tetrazolium bromide (MTT) assay was used to test the cytotoxicity of the produced SeNPs on three tested cell lines. The cells were cultured in RPMI-1640 with 10% FCS and penicillin/streptomycin;  $6 \cdot 10^3$  cells were seeded in 96-well plates and incubated for 24 h at 37  $^{\circ}\text{C}$  under  $\text{CO}_2$ . Then, supernatant from the grown cells was collected after 24 h, and different quantities of SeNPs (10 to 240  $\mu\text{g}/\text{mL}$ ) were diluted with the growth medium and added to each well. After 48 h of incubation, 20  $\mu\text{L}$  of MTT (5 mg/mL) was added to each well and incubated for 4 h. Finally, the purple-colored formazan crystals were dissolved in a 200  $\mu\text{L}$  DMSO solution. A spectrophotometer (Biotek Instruments; USA) was used to measure the optical density of each well at 590 nm. The % cell viability was assessed by the following equation [28,33,34]:

$$\text{Cell viability} = \frac{\text{The optical density of the sample well}}{\text{The optical density of control well}} \quad (1)$$

### 2.6. Catalytic activity of synthesized B@SeNPs

Metal nanoparticles could be used to catalyze chemical reactions that would otherwise be impossible to achieve. The catalytic effect of the B@SeNPs produced was tested on methylene blue as a toxic dye using  $\text{NaBH}_4$ ; 30  $\mu\text{L}$  of 10 mM MB solution was mixed with 5.77 mL of  $\text{H}_2\text{O}$  and 200  $\mu\text{L}$  of freshly made 0.1 M  $\text{NaBH}_4$  solution. Then 70  $\mu\text{L}$  of colloidal SeNPs (1110  $\mu\text{g}/\text{mL}$ ) was added to the prepared mixture containing MB and  $\text{NaBH}_4$ . There was also a blank sample made without SeNPs. The color of the SeNPs-containing sample progressively faded from deep to light blue before becoming colorless. The MB reduction was measured using a UV-vis spectrophotometer

at regular time intervals. The test was carried out at room temperature.

The pseudo-first-order equation (2) was used to monitor the MB's degradation rate;  $A_t$  and  $A_0$  were the absorbance at interval times and time 0, respectively [31].

$$\ln \left( \frac{A}{A_0} \right) = -kt \quad (2)$$

### 2.7. Statistical analysis

All experiments were carried out in triplicate and data were represented as (mean value $\pm$ SD). All statistical analyses were performed by one-way ANOVA at  $p < 0.05$  using GraphPad prism software.

## 3. Results and discussion

### 3.1. Characterization of green synthesized B@SeNPs

Biomolecules in the aqueous extract of *H. esculentus* reduced the  $\text{Na}_2\text{SeO}_3$  salt solution to SeNPs. The solution color changed from colorless to reddish after 48 h; this is the surface plasmon resonance effect (SPR). Various temperatures (25, 45, and 75  $^{\circ}\text{C}$ ) and pH values (6 (extract pH), 10, and 12) were studied to optimize the synthesis conditions of SeNPs using *H. esculentus*; Based on the results, the reddish color of the mixture occurred at 45-50  $^{\circ}\text{C}$  and the extract pH (pH = 6), as demonstrated in Figure 2. Other conditions did not affect the color change. Furthermore, the absorbance of the solution was measured using a UV-visible spectrophotometer with a wavelength range of 200 to 800 nm (Figure 2). *Cassia auriculata*-mediated SeNPs had a UV-intensive peak at 252 nm [18]. Ramamurthy and colleagues used Fenugreek extract to make SeNPs, with a distinctive peak between 200 and 400 nm [35]. The solution containing SeNPs was centrifuged after the washing process and dried in an oven before being used for additional analysis.

The particle length and form of SeNPs have been predicted with the aid of TEM images. Figure 3 indicates the implied length of SeNPs (62 nm), with sphere polydispersed debris; this is attributed to the biomolecules in the plant extract; that perform as capping, reducing, and stabilizing agents. SEM images were used to examine the shape and surface characteristics of SeNPs. The SEM picture of SeNPs with variable size and homogeneous rounded form is shown in Figure 4. Additionally, the average size obtained from the SEM image was 50.1 nm; the histogram is presented in Figure 5. The SeNPs synthesized by *Allium paradoxum* extract displayed semi-spherical SeNPs with an average size of 37.5 nm [31].

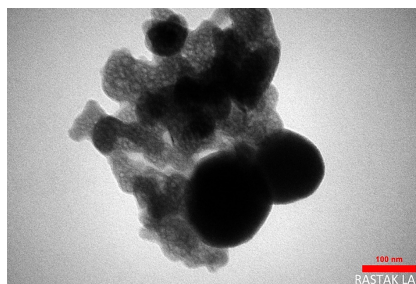


Figure 3. TEM image of green synthesized B@SeNPs.

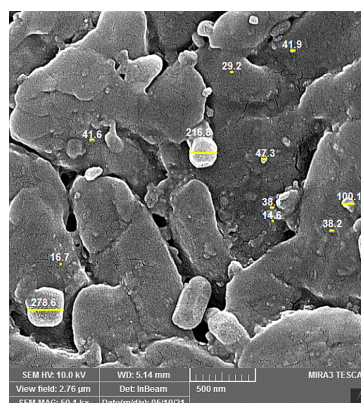


Figure 4. The SEM image of green synthesized B@SeNPs.

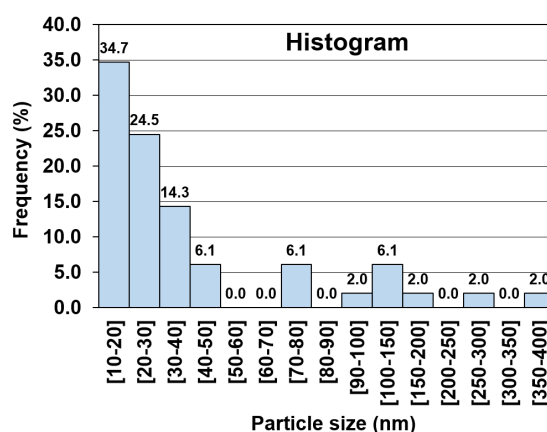


Figure 5. Histogram obtained from the SEM image of green synthesized B@SeNPs.

SEM and TEM images of SeNPs using *Mucuna pruriens* seed powder showed that the NPs produced had a spherical shape and a homogeneous dispersion in a size range of about 100-110 nm [36]. Green SeNPs produced by the *Solanum nigrum* fruit extract were spherical with a particle diameter of 87 nm [37]. TEM micrographs of the biogenic SeNPs of *Spirulina platensis* presented spherical shapes with a mean size of  $79.40 \pm 44.26$  nm [38].

As seen in Figure 6, EDX analysis was used to verify the elemental summary of SeNPs and its ability to indicate the purity of the offered SeNPs. SeNPs exhibited typical Se absorption maxima at 1.39 keV. The high amount of selenium demonstrates the purity of this element (Se = 81.37 %). The presence of carbon at 0.29 keV and oxygen at 0.54 keV indicates the existence of alkyl chain stabilizers.

SeNPs were discovered to have a particle size and distribution of 266.3 nm (Figure 7). The DLS size range of the synthesized SeNPs was found to be significantly larger than the TEM size range. Because DLS measures the hydrodynamic

diameter of the SeNPs when they are surrounded by water molecules, it is possible that this is the source of the enormous size of the capped formulation. The zeta potential that showed the stability of SeNPs was found to be -51.3 mV (Figure 8). The zeta potential of *S. platensis*-mediated SeNPs was  $-32.9 \pm 8.12$  mV [38]. Furthermore, SeNPs synthesized by aqueous extract of *Portulaca oleracea* indicated a zeta potential of -43.8 mV [39].

The synthesized SeNPs were crystallized according to the XRD pattern of the sample (Figure 9). The peaks at 23.45, 29.65, 41.20, 43.70, 45.35, 51.75, 56.20, 61.65, and 65.45 ° were labelled in Bragg's appearances as (100), (101), (110), (102), (111), (201), (112), (202), and (210), respectively. All peaks can be matched with SeNPs JCPDS (Joint Committee on Powder Diffraction Standards) (JCPDS File No. 06-0362). The result indicates that the bioprepared SeNPs produced the hexagonal phase crystalline form [40]. The determined size by the Debye-Scherrer equation was 34.8 nm.

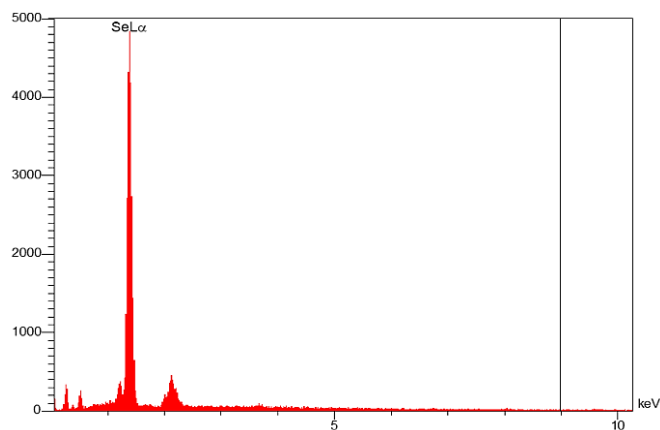


Figure 6. EDX analysis of green prepared B@SeNPs.

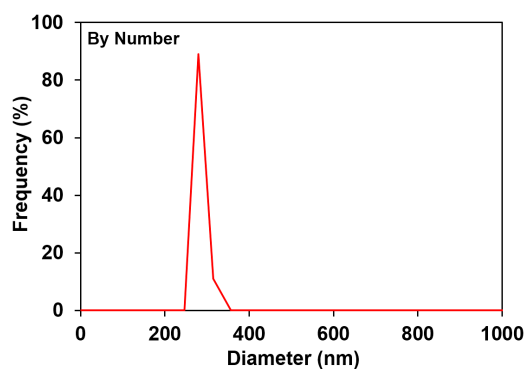


Figure 7. DLS graph of the synthesized B@SeNPs.

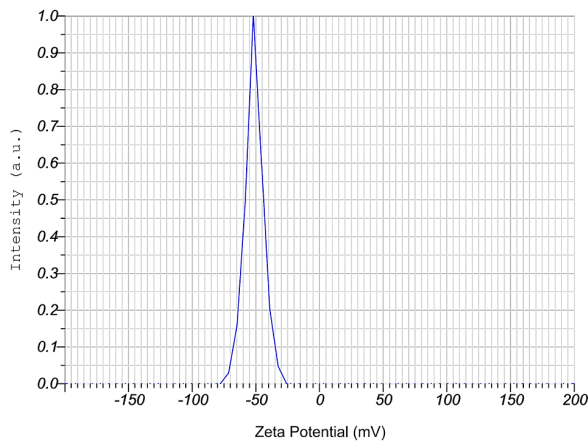


Figure 8. Zeta potential of the synthesized B@SeNPs.

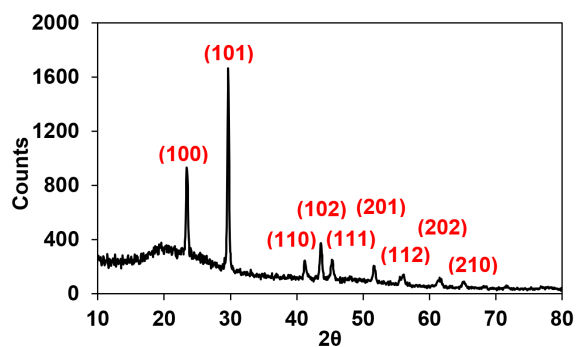


Figure 9. The XRD pattern of the synthesized B@SeNPs.



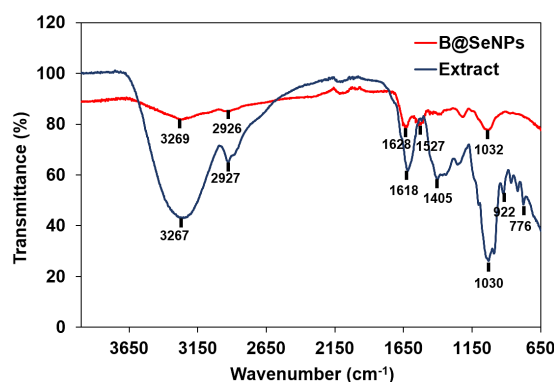
**Table 1.** The MIC and MBC values obtained from biosynthesized B@SeNPs against several ATCC strains.

Bacteria	ATCC	B@SeNPs		Extract	Ciprofloxacin
		MIC ( $\mu\text{g/mL}$ )	MBC ( $\mu\text{g/mL}$ )	MIC ( $\mu\text{g/mL}$ )	MIC ( $\mu\text{g/mL}$ )
<i>S. aureus</i>	ATCC 29213	69.35	138.75	>2500	0.21
<i>E. faecalis</i>	ATCC 29212	17.34	138.75	>2500	0.21
<i>P. aeruginosa</i>	ATCC 27853	138.75	1110	>2500	0.3
<i>A. baumannii</i>	ATCC 19606	34.7	1110	>2500	0.25
<i>E. coli</i>	ATCC 25922	138.75	555	>2500	0.1
<i>K. pneumoniae</i>	ATCC 700603	69.35	555	>2500	0.1
<i>P. mirabilis</i>	ATCC 25933	17.34	277.5	>2500	0.1

**Table 2.** The MIC and MBC values obtained from biosynthesized B@SeNPs against several clinically isolated strains\*.

Bacteria	B@SeNPs		Extract	Susceptibility to antibacterial agents										
	MIC ( $\mu\text{g/mL}$ )	MBC ( $\mu\text{g/mL}$ )	MIC ( $\mu\text{g/mL}$ )	M	V	O	T	G	P	Cl	CE	E	CM	AK
<i>S. aureus</i> (VRSA)	138.75	555	>2500	R	R	R	S	R	R	R	R	R	R	R
<i>S. aureus</i> (MRSA)	138.75	555	>2500	R	R	R	S	R	R	R	R	R	R	R
<i>E. faecalis</i>	138.75	555	>2500	S	R	R	R	R	R	S	R	R	R	R
<i>P. aeruginosa</i>	277.5	1110	>2500	R	R	R	R	R	R	R	R	R	R	R
<i>A. baumannii</i>	277.5	1110	>2500	R	R	R	R	R	R	R	R	R	R	R
<i>E. coli</i>	277.5	1110	>2500	R	R	R	R	R	R	R	R	R	R	R
<i>K. pneumoniae</i>	277.5	555	>2500	R	R	R	R	R	R	R	R	R	R	R
<i>P. mirabilis</i>	277.5	1110	>2500	R	R	R	R	R	R	R	R	R	R	R

\* R, resistant; S, susceptible; M, Meticillin; V, Vancomycin; O, Oxacillin; T, Tetracycline; G, Gentamicin; P, Penicillin; Cl, Ciprofloxacin; CE, Ceftazidime; E, Erythromycin; CM, Clindamycin; A, Amikacin; MRSA, methicillin resistant *Staphylococcus aureus*; VRSA, Vancomycin resistant *Staphylococcus aureus*.

**Figure 10.** The FT-IR of the synthesized B@SeNPs.

These results were consistent with the XRD pattern of SeNPs prepared using *Diospyros montana* extract, which presented the hexagonal structure of SeNPs [41].

FT-IR analysis was used to identify the molecular interaction between the extract and G@SeNPs. As shown in Figure 10, the FT-IR spectrum of the extract exhibited absorption bands at 3267, 2927, 1618, 1405, 1030, 922, and 776  $\text{cm}^{-1}$ . Moreover, the spectrum of synthesized SeNPs showed absorption peaks at 3269, 2926, 1628, 1527, and 1032  $\text{cm}^{-1}$ . The broad peak at 3267 and 2927  $\text{cm}^{-1}$  corresponded to the stretching of O-H and the asymmetric stretching of the C-H bonds, respectively [42]. The peaks at 1618 and 1405  $\text{cm}^{-1}$  are assigned to carbonyl stretching bands (amides) [43] and -OH bonds of carboxylates [18,42,44,45]. Another peak at 1030  $\text{cm}^{-1}$  was related to C-N (stretching vibration of primary amines) [18,42]. According to the FT-IR data, the intensity of all bonds had decreased in the SeNPs spectrum, which could be attributed to the binding of SeNPs to the functional groups of the extract.

### 3.2. Antibacterial activity of SeNPs against ATCC strains and clinically isolated strains

This study used two series of ATCC bacteria and clinically obtained bacteria to test their susceptibility to prepared B@SeNPs (Tables 1 and 2). The antibacterial properties of B@SeNPs produced in the presence of *H. esculentus* extract were tested against Gram positive and Gram-negative bacteria. Various concentrations of B@SeNPs (277.5 to 0.27  $\mu\text{g/mL}$ ) and *H. esculentus* extract (2500 to 312.5  $\mu\text{g/mL}$ ) were used to treat test pathogens. The MIC assay was performed using the broth dilution method for both MDR and ATCC strains listed in Tables

1 and 2. The antibacterial activity of B@SeNPs revealed that when the concentration of B@SeNPs increased, the MIC value of bacteria decreased. As shown, *E. faecalis* (ATCC) and *P. mirabilis* (ATCC) were found to be the most sensitive to B@SeNPs, with a MIC value of 17.34  $\mu\text{g/mL}$ . Furthermore, clinically isolated strains *E. faecalis*, *S. aureus* (VRSA), and *S. aureus* (MRSA) exhibited the lowest MIC value of 138.75  $\mu\text{g/mL}$ . *S. nigrum*-mediated SeNPs did not inhibit *S. aureus*, while it showed a MBC value of  $50 \pm 1.76$   $\text{mg/mL}$  against *E. coli* [37]. In another study, green SeNPs from *Lysinibacillus* sp. N0SK inhibited the biofilm of *P. aeruginosa* compared to untreated samples [46]. The antibacterial investigation of SeNPs from Vitamin C showed a dose-dependent manner against *E. coli*, *P. aeruginosa*, *S. aureus*, and *S. epidermidis* [47].

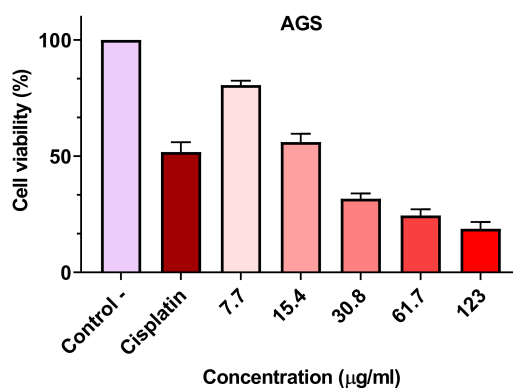
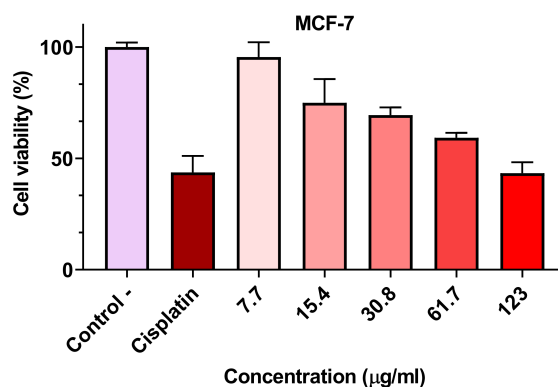
According to many sources, the antimicrobial activity of SeNPs is primarily due to the generation of reactive oxygen species (ROS), which causes the phospholipid bilayer to be disrupted, allowing the SeNPs to interact with intracellular proteins and inactivate them or react with the sulphhydryl and thiol groups that exist in membrane proteins, causing them to denaturise. Furthermore, ROS causes cell death by disrupting the protein synthesis cycle, intervening in the respiratory or food metabolic pathways, and affecting DNA replication [48,49].

### 3.3. Antifungal activity of SeNPs against fungi strains resistant to itraconazole

The antifungal effect of SeNPs was evaluated against eight fungus strains resistant to itraconazole by the micro broth dilution method.

**Table 3.** The MIC value achieved from biosynthesized B@SeNPs against several fungi isolates.

The fungi isolates tasted	B@SeNPs	Itraconazole	Extract
	MIC ( $\mu\text{g/mL}$ )	MIC ( $\mu\text{g/mL}$ )	MIC ( $\mu\text{g/mL}$ )
<i>Aspergillus fumigatus</i> (IFRC 1649)	R	$\geq 16$	>2500
<i>Aspergillus fumigatus</i> (IFRC 1505)	R	$\geq 16$	>2500
<i>Trichophyton mentagrophytes</i> (FR1 22130)	R	$\geq 16$	>2500
<i>Trichophyton mentagrophytes</i> (FR5 22130)	R	$\geq 16$	>2500
<i>Fusarium proliferatum</i> (IFRC 1871)	R	$\geq 16$	>2500
<i>Fusarium equiseti</i> (IFRC 1872)	R	$\geq 16$	>2500
<i>Candida albicans</i> (IFRC 1873)	138.75	$\geq 16$	>2500
<i>Candida albicans</i> (IFRC 1874)	R	$\geq 16$	>2500

**Figure 11.** *In-vitro* cytotoxicity of B@SeNPs at different concentrations against AGS cell line.**Figure 12.** *In-vitro* cytotoxicity of B@SeNPs at different concentrations on MCF-7 cell line.

The minimal inhibitory concentration (MIC) was visually determined, which means it cannot be quantified. Our synthesized SeNPs at concentrations 555-0.54  $\mu\text{g/mL}$  did not show antifungal activity against tested fungi strains except *C. albicans* (IFRC 1873), which had a MIC value of 138.75  $\mu\text{g/mL}$  (Table 3). Furthermore, the antifungal activity of the extract was examined at concentrations of 2500 to 312.5  $\mu\text{g/mL}$ , showing growth in all wells. The reference antibiotic was itraconazole. The MIC values of the *Allium paradoxum*-mediated SeNPs were 0.68  $\mu\text{g/mL}$  against all fungal strains similar to those tested in our study, except for two strains of *C. albicans*. In fact, SeNPs were resistant to *C. albicans* [31]. In another investigation, the SeNPs manufactured by *Bacillus* species Msh-1 displayed MIC values of 70  $\mu\text{g/ml}$  and 100  $\mu\text{g/ml}$  against *C. albicans* and *A. fumigatus*, respectively [50].

### 3.4. Anticancer activity of SeNPs

Chemotherapy is a well-known cancer treatment method, and employing targeted NPs to deliver chemotherapeutic medications to cancer patients has several advantages. Because drugs associated with NPs can penetrate deeper into organs, NPs are used in cancer drug delivery. Interestingly, various

research organizations have concentrated on developing a promising source of new therapeutic molecules for cancer treatment [1]. In this work, the *in vitro* cytotoxicity of SeNPs was investigated against human gastric cancer (AGS), human breast adenocarcinoma (MCF-7), and human non-tumorigenic lung epithelial cell line (Beas) using the MTT assay. Cells were treated with five different concentrations of SeNPs (123, 61.7, 30.8, 15.4, and 7.7  $\mu\text{g/mL}$ ) at 48 h. The results of the MTT test revealed that SeNPs had significant effects on AGS and MCF-7; The  $\text{IC}_{50}$  values on AGS and MCF-7 were found to be 20.46 and 88.43  $\mu\text{g/mL}$ , respectively (Figures 11 and 12). Furthermore, our synthesized nanoparticles exhibited excellent safety in the normal cell line, Beas, at the highest concentration (123  $\mu\text{g/mL}$ ) (Figure 13). Therefore, the prepared B@SeNPs showed high cytotoxicity against the AGS and MCF-7 cell lines. This synthetic method provides many advantages, including simplicity, cost-effectiveness, and compatibility for pharmaceutical and medical applications. In a study in 2019,  $\text{IC}_{50}$  values of 150.87, 392.57, and 252.44  $\mu\text{g/mL}$  were discovered on the Caco2, HepG-2 and MCF-7 cell lines for *M. Oleifera* leaves mediated SeNPs, respectively [1]. The  $\text{IC}_{50}$  value for SeNPs produced by Vitamin C on MCF-7 cancer cells was calculated at 23.20  $\mu\text{g/mL}$  [51].

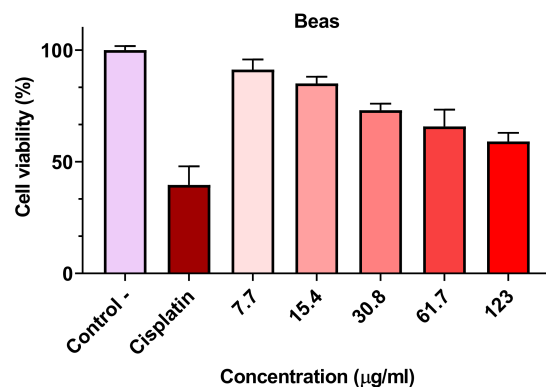


Figure 13. *In-vitro* cytotoxicity of B@SeNPs at different concentrations on normal cell lines of Beas.

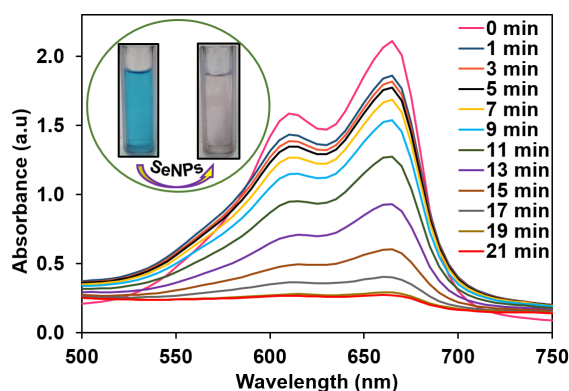


Figure 14. The catalytic reduction of MB using 70  $\mu\text{L}$  B@SeNPs (1110  $\mu\text{g/mL}$ ) in the presence of  $\text{NaBH}_4$ .

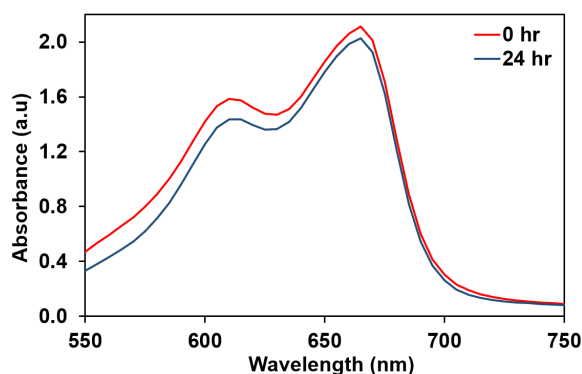


Figure 15. The reduction of MB using  $\text{NaBH}_4$ .

### 3.5. Catalytic effect of B@SeNPs on methylene blue

The methylene blue reduction process by  $\text{NaBH}_4$  was used as a model reaction to evaluate the catalytic activity of biosynthesized B@SeNPs. This dye is a basic aniline dye, also identified as methylthionium chloride, which has a wide range of applications in biology and chemistry, as well as a stain and medication. When MB is oxidized, it is blue, but when it is reduced, it becomes colorless leucomethylene blue [52]. In an aqueous solution, MB shows an absorption maxima band around 665 nm due to the  $\pi \rightarrow \pi^*$  and  $n \rightarrow \pi^*$  transitions. Based on the result, the UV-Vis spectra of MB reduction by  $\text{NaBH}_4$  in the presence of produced catalyst SeNPs are shown in Figure 14. The MB reduction by  $\text{NaBH}_4$  in the lack of the SeNPs was shown in Figure 15. Obviously, in the absence of B@SeNPs, the dye reduction rate was substantially slower than that in their presence. The reduction was accomplished in 21 min in the presence of 70  $\mu\text{L}$  of B@SeNPs. Additionally, the degradation

percentage of MB in time intervals was presented in Figure 16. This result demonstrated that adding B@SeNPs in the right amount to the MB reduction process made it more efficient. This reduction reaction was found to be pseudo-first order, and the rate constant was calculated as  $0.1023 \text{ min}^{-1}$ . The spectra in Figure 17 exhibited  $\ln A_t/A_0$  versus time for MB reduction using B@SeNPs at room temperature. The biosynthesized SeNPs using the leaf extract of *Ficus benghalensis* exhibited a degradation of 57.63% in 40 min with a rate constant of  $0.02162 \text{ s}^{-1}$  against the MB dye [3]. In another study, eco-friendly and rapidly fabricated SeNPs through aqueous extracts of *Ceropegia bulbosa tuber* presented effective photocatalytic activity against MB using a halogen lamp with 96% degradation [53]. In addition, *Withania somnifera*-mediated SeNPs decreased the MB peak intensity during 30 min under solar light [14].



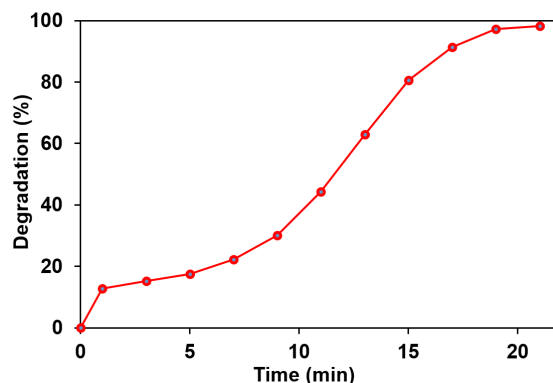


Figure 16. Degradation percentage of MB reduction using B@SeNPs and NaBH<sub>4</sub>.

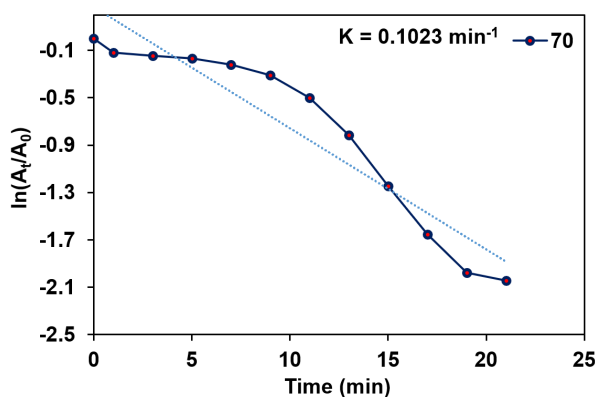


Figure 17. The calculation of the rate constant by plotting  $\ln(A_t/A_0)$  vs time.

Based on the data, biosynthesized colloidal B@SeNPs were applied as an excellent green catalyst, mediating electron transfer during the MB reduction by NaBH<sub>4</sub>. The bond dissociation energy (BDE) is a significant factor in the breaking and/or production of new bonds during chemical reactions. In the interaction between MB and NaBH<sub>4</sub>, NaBH<sub>4</sub> operates as a donor and MB as an acceptor, resulting in electron transfer. The introduction of selenium nanocatalysts to the reaction mixture acted as a possible intermediary between the MB and BH<sub>4</sub> ions. It initially reduced the BDE and increased the efficiency of electron transport between them. In the presence of SeNPs, the rate of MB reduction by NaBH<sub>4</sub> was enhanced. In the catalytic reduction of organic color, colloidal SeNPs produced from readily available extracts exhibited encouraging results [52].

#### 4. Conclusion

This work used an aqueous extract of *H. esculentus* to produce SeNPs without the use of harmful or dangerous chemicals. In this green synthesis process, the extract of *H. esculentus* serves as a natural reducing, capping, and stabilizing agent. The existence of various functional groups in *H. esculentus* was indicated by FT-IR findings, which influenced the synthesis and stabilization of B@SeNPs. The color of the reaction medium changed from colorless to brick red, showing the synthesis of Se<sup>0</sup>. The production of crystalline B@SeNPs with an average size of 34.8 nm was confirmed using the XRD pattern. The produced NPs were found to be of atomic Se using EDX. SEM and TEM studies were used to document the morphology of the synthesized B@SeNPs. In addition, they have a spherical shape with an average size of 62 nm in the TEM image. Catalytic analysis revealed that B@SeNPs are capable of degrading methylene blue dye in the presence of NaBH<sub>4</sub> and visible light. As a result, B@SeNPs could be used in water

treatment. Furthermore, the anticancer activity of B@SeNPs generated in an environmentally friendly manner using the plant-mediated method was investigated. B@SeNPs have been shown to be effective against two types of human cancer cells (AGS and MCF-7 cells) while remaining relatively safe for normal cell Beas. The IC<sub>50</sub> values of 20.46 and 88.43 μg/mL suggest that B@SeNPs are powerful anticancer agents with high safety in normal cells that suppress the growth of both types of cancers. Furthermore, the biofabricated SeNPs revealed moderate antibacterial activity against two types of bacterial strains (ATCC and clinically isolated), and they did not show antifungal activity against some fungi strains. The green synthesis of B@SeNPs could be a useful method in biomedical applications.

#### Acknowledgements

This research was supported by a grant from the research council of Mazandaran University of Medical Sciences, Iran (Grant No. 10555).

#### Disclosure statement

Conflict of interest: The authors declare that they have no conflict of interest. Ethical approval: All ethical guidelines have been adhered. Sample availability: Samples of the compounds are available from the author. Declaration of competing interests: The authors declare that they have no known competing financial interests or personal relationships that could have appeared to influence the work reported in this paper.

#### CRedit authorship contribution statement

Conceptualization: Mohammad Ali Ebrahimzadeh; Methodology: Mohammad Ali Ebrahimzadeh, Fatemeh Sadeghi Lalerdi, Mina Moradosmarein; Formal analysis: Mohammad Ali Ebrahimzadeh; Investigation: Mohammad Ali Ebrahimzadeh, Fatemeh Sadeghi Lalerdi; Resources: Seyedeh Roya Alizadeh; Funding: Seyedeh Roya Alizadeh; Supervision: Seyedeh Roya Alizadeh;

Writing - Original Draft: Mohammad Ali Ebrahimzadeh, Fatemeh Sadeghi Lalerdi, Mina Moradsomarein, Seyedeh Roya Alizadeh; Review and Editing: Seyedeh Roya Alizadeh. All authors have read and agreed to the published version of the manuscript.

## ORCID and Email

Mohammad Ali Ebrahimzadeh

 [zadeh20@gmail.com](mailto:zadeh20@gmail.com)

 <https://orcid.org/0000-0002-8769-9912>

Mina Moradsomarein

 [minamrds97@gmail.com](mailto:minamrds97@gmail.com)


 <https://orcid.org/0000-0002-5374-1940>

Fatemeh Sadeghi Lalerdi

 [fatemehsadeghi132@yahoo.com](mailto:fatemehsadeghi132@yahoo.com)

 <https://orcid.org/0000-0001-5518-0051>

Seyedeh Roya Alizadeh

 [r.alizadeh.2019@gmail.com](mailto:r.alizadeh.2019@gmail.com)

 [ro.alizadeh@mazums.ac.ir](mailto:ro.alizadeh@mazums.ac.ir)

 <https://orcid.org/0000-0001-7435-4635>

## References

- Hassanien, R.; Abed-Elmageed, A. A. I.; Husein, D. Z. Eco-friendly approach to synthesize selenium nanoparticles: Photocatalytic degradation of sunset yellow azo dye and anticancer activity. *ChemistrySelect* **2019**, *4*, 9018–9026.
- Vuppala, V.; Motappa, M. G.; Venkata, S. S.; Sadashivaiah, P. H. Photocatalytic degradation of methylene blue using a zinc oxide-cerium oxide catalyst. *Eur. J. Chem.* **2012**, *3*, 191–195.
- Tripaht, R. M.; Hameed, P.; Rao, R. P.; Shrivastava, N.; Mittal, J.; Mohapatra, S. Biosynthesis of highly stable fluorescent selenium nanoparticles and the evaluation of their photocatalytic degradation of dye. *Bionanoscience* **2020**, *10*, 389–396.
- Kandisa, R. V.; Saibaba KV, N. Dye removal by adsorption: A review. *J. Bioremediat. Biodegrad.* **2016**, *07*, 371.
- Jassim, A. M. N.; Al-Kazaz, F. F. M. Biochemical study for gold and silver nanoparticles on thyroid hormone levels in saliva of patients with chronic renal failure. *Eur. J. Chem.* **2013**, *4*, 353–359.
- Agarwal, M.; Singh Bhadwal, A.; Kumar, N.; Shrivastav, A.; Raj Shrivastav, B.; Pratap Singh, M.; Zafar, F.; Mani Tripathi, R. Catalytic degradation of methylene blue by biosynthesized copper nanoflowers using *F. benghalensis* leaf extract. *IET Nanobiotechnol.* **2016**, *10*, 321–325.
- Tripaht, R. M.; Shrivastav, B. R.; Shrivastav, A. Antibacterial and catalytic activity of biogenic gold nanoparticles synthesized by *Trichoderma harzianum*. *IET Nanobiotechnol.* **2018**, *12*, 509–513.
- Shirzadi-Ahodashi, M.; Mizwari, Z. M.; Hashemi, Z.; Rajabalipour, S.; Ghoreishi, S. M.; Mortazavi-Derazkola, S.; Ebrahimzadeh, M. A. Discovery of high antibacterial and catalytic activities of biosynthesized silver nanoparticles using *C. fruticosus* (CF-AgNPs) against multi-drug resistant clinical strains and hazardous pollutants. *Environ. Technol. Innov.* **2021**, *23*, 101607.
- Shirzadi-Ahodashi, M.; Hashemi, Z.; Mortazavi, Y.; Khormali, K.; Mortazavi-Derazkola, S.; Ebrahimzadeh, M. A. Discovery of high antibacterial and catalytic activities against multi-drug resistant clinical bacteria and hazardous pollutants by biosynthesized silver nanoparticles using *Stachys inflata* extract (AgNPs@SI). *Colloids Surf. A Physicochem. Eng. Asp.* **2021**, *617*, 126383.
- Hashemi, Z.; Shirzadi-Ahodashi, M.; Mortazavi-Derazkola, S.; Ebrahimzadeh, M. A. Sustainable biosynthesis of metallic silver nanoparticles using barberry phenolic extract: Optimization and evaluation of photocatalytic, in vitro cytotoxicity, and antibacterial activities against multidrug-resistant bacteria. *Inorg. Chem. Commun.* **2022**, *139*, 109320.
- Rayman, M. P. Selenium and human health. *Lancet* **2012**, *379*, 1256–1268.
- Pyrzynska, K.; Sentkowska, A. Biosynthesis of selenium nanoparticles using plant extracts. *J. Nanostructure Chem.* **2022**, *12*, 467–480.
- Krishnan, M.; Ranganathan, K.; Maadhu, P.; Thangavelu, P.; Kundan, S.; Arjunan, N. Leaf extract of *Dillenia indica* as a source of selenium nanoparticles with larvicidal and antimicrobial potential toward vector mosquitoes and pathogenic microbes. *Coatings* **2020**, *10*, 626.
- Alagesan, V.; Venugopal, S. Green synthesis of selenium nanoparticle using leaves extract of *Withania somnifera* and its biological applications and photocatalytic activities. *Bionanoscience* **2019**, *9*, 105–116.
- Ameri, A.; Shakibaie, M.; Ameri, A.; Faramarzi, M. A.; Amir-Heidari, B.; Foroootanfar, H. Photocatalytic decolorization of bromothymol blue using biogenic selenium nanoparticles synthesized by terrestrial actinomycete *Streptomyces griseobrunneus* strain FSHH12. *Desalination Water Treat.* **2016**, *57*, 21552–21563.
- Kumar, A.; Prasad, B.; Manjhi, J.; Prasad, K. S. Antioxidant activity of selenium nanoparticles biosynthesized using a cell-free extract of *Geobacillus*. *Toxicol. Environ. Chem.* **2020**, *102*, 556–567.
- Amiri, H.; Hashemy, S. I.; Sabouri, Z.; Javid, H.; Darroudi, M. Green synthesized selenium nanoparticles for ovarian cancer cell apoptosis. *Res. Chem. Intermed.* **2021**, *47*, 2539–2556.
- Anu, K.; Devanesan, S.; Prasanth, R.; AlSalhi, M. S.; Ajithkumar, S.; Singaravelu, G. Biogenesis of selenium nanoparticles and their anti-leukemia activity. *J. King Saud Univ. Sci.* **2020**, *32*, 2520–2526.
- Vahidi, H.; Barabadi, H.; Saravanan, M. Emerging selenium nanoparticles to combat cancer: A systematic review. *J. Cluster Sci.* **2020**, *31*, 301–309.
- Wadhvani, S.; Gorain, M.; Banerjee, P.; Shedbalkar, U.; Singh, R.; Kundu, G.; Chopade, B. A. Green synthesis of selenium nanoparticles using *Acinetobacter* sp. SW30: optimization, characterization and its anticancer activity in breast cancer cells. *Int. J. Nanomedicine* **2017**, *12*, 6841–6855.
- Pandey, S.; Awasthee, N.; Shekher, A.; Rai, L. C.; Gupta, S. C.; Dubey, S. K. Biogenic synthesis and characterization of selenium nanoparticles and their applications with special reference to antibacterial, antioxidant, anticancer and photocatalytic activity. *Bioprocess Biosyst. Eng.* **2021**, *44*, 2679–2696.
- Ebrahimzadeh, M. A.; Nabavi, S. F.; Nabavi, S. M.; Eslami, B. Antihypoxic and antioxidant activity of *Hibiscus esculentus* seeds. *Grasas Aceites* **2010**, *61*, 30–36.
- Sorapong, B. Okra (*Abelmoschus esculentus* (L.) Moench) as a valuable vegetable of the world. *Ratar. Povrt.* **2012**, *49*, 105–112.
- Saifullah, M.; Rabbani, M. G. Evaluation and characterization of okra (*Abelmoschus esculentus* L. Moench.) genotypes. *SAARC Journal of Agriculture* **2009**, *7*, 91–98.
- Shui, G.; Peng, L. L. An improved method for the analysis of major antioxidants of *Hibiscus esculentus* Linn. *J. Chromatogr. A* **2004**, *1048*, 17–24.
- Chowdhury, N. R.; MacGregor-Ramiasa, M.; Zilm, P.; Majewski, P.; Vasilev, K. "Chocolate" silver nanoparticles: Synthesis, antibacterial activity and cytotoxicity. *J. Colloid Interface Sci.* **2016**, *482*, 151–158.
- Mortazavi-Derazkola, S.; Ebrahimzadeh, M. A.; Amiri, O.; Goli, H. R.; Rafiei, A.; Kardan, M.; Salavati-Niasari, M. Facile green synthesis and characterization of *Crategeus microphylla* extract-capped silver nanoparticles (CME@Ag-NPs) and its potential antibacterial and anticancer activities against AGS and MCF-7 human cancer cells. *J. Alloys Compd.* **2020**, *820*, 153186.
- Hashemi, Z.; Mohammadyan, M.; Naderi, S.; Fakhar, M.; Biparva, P.; Akhtari, J.; Ebrahimzadeh, M. A. Green synthesis of silver nanoparticles using *Ferula persica* extract (Fp-NPs): Characterization, antibacterial, antileishmanial, and in vitro anticancer activities. *Mater. Today Commun.* **2021**, *27*, 102264.
- Shirzadi-Ahodashi, M.; Mizwari, Z. M.; Mohammadi-Aghdam, S.; Ahmadi, S.; Ali Ebrahimzadeh, M.; Mortazavi-Derazkola, S. Optimization and evaluation of anticancer, antifungal, catalytic, and antibacterial activities: Biosynthesis of spherical-shaped gold nanoparticles using *Pistacia vera* hull extract (AuNPs@PV). *Arab. J. Chem.* **2023**, *16*, 104423.
- Nidhin; Saneha; Hans, S.; Varghese, A.; Fatima, Z.; Hameed, S. Studies on the antifungal activity of biotemplated gold nanoparticles over *Candida albicans*. *Mater. Res. Bull.* **2019**, *119*, 110563.
- Alizadeh, S. R.; Seyedabadi, M.; Montazeri, M.; Khan, B. A.; Ebrahimzadeh, M. A. Allium paradoxum extract mediated green synthesis of SeNPs: Assessment of their anticancer, antioxidant, iron chelating activities, and antimicrobial activities against fungi, ATCC bacterial strains, Leishmania parasite, and catalytic reduction of methylene blue. *Mater. Chem. Phys.* **2023**, *296*, 127240.
- Hashemi, Z.; Mizwari, Z. M.; Mohammadi-Aghdam, S.; Mortazavi-Derazkola, S.; Ali Ebrahimzadeh, M. Sustainable green synthesis of silver nanoparticles using *Sambucus ebulus* phenolic extract (AgNPs@SEE): Optimization and assessment of photocatalytic degradation of methyl orange and their in vitro antibacterial and anticancer activity. *Arab. J. Chem.* **2022**, *15*, 103525.
- Al Jahdaly, B. A.; Al-Radadi, N. S.; Eldin, G. M. G.; Almahri, A.; Ahmed, M. K.; Shoueir, K.; Janowska, I. Selenium nanoparticles synthesized using an eco-friendly method: dye decolorization from aqueous solutions, cell viability, antioxidant, and antibacterial effectiveness. *J. Mater. Res. Technol.* **2021**, *11*, 85–97.
- Hashemi, Z.; Ebrahimzadeh, M. A.; Biparva, P.; Mortazavi-Derazkola, S.; Goli, H. R.; Sadeghian, F.; Kardan, M.; Rafiei, A. Biogenic silver and zero-valent iron nanoparticles by *Feijoa*: Biosynthesis, characterization, cytotoxic, antibacterial and antioxidant activities. *Anticancer Agents Med. Chem.* **2020**, *20*, 1673–1687.
- Ramamurthy, C.; Sampath, K. S.; Arunkumar, P.; Kumar, M. S.; Sujatha, V.; Premkumar, K.; Thirunavukkarasu, C. Green synthesis and characterization of selenium nanoparticles and its augmented cytotoxicity with doxorubicin on cancer cells. *Bioprocess Biosyst. Eng.* **2013**, *36*, 1131–1139.

- [36]. Menon, S.; Agarwal, H.; Shanmugam, V. K. Catalytic degradation of industrial dyes using biosynthesized selenium nanoparticles and evaluating its antimicrobial activities. *Sustain. Environ. Res.* **2021**, *31*, 2.
- [37]. Saranya, T.; Ramya, S.; Kavitha, K.; Paulpandi, M.; Cheon, Y.-P.; Harysh Winstler, S.; Balachandar, V.; Narayanasamy, A. Green synthesis of selenium nanoparticles using *Solanum nigrum* fruit extract and its anti-cancer efficacy against triple negative breast cancer. *J. Cluster Sci.* **2022**, <https://doi.org/10.1007/s10876-022-02334-2>.
- [38]. Abbas, H. S.; Abou Baker, D. H.; Ahmed, E. A. Cytotoxicity and antimicrobial efficiency of selenium nanoparticles biosynthesized by *Spirulina platensis*. *Arch. Microbiol.* **2021**, *203*, 523–532.
- [39]. Fouda, A.; Al-Otaibi, W. A.; Saber, T.; AlMotwaa, S. M.; Alshallah, K. S.; Elhady, M.; Badr, N. F.; Abdel-Rahman, M. A. Antimicrobial, antiviral, and in-vitro cytotoxicity and mosquitocidal activities of *Portulaca oleracea*-based green synthesis of selenium nanoparticles. *J. Funct. Biomater.* **2022**, *13*, 157.
- [40]. Srivastava, N.; Mukhopadhyay, M. Biosynthesis and structural characterization of selenium nanoparticles mediated by *Zooglea ramigera*. *Powder Technol.* **2013**, *244*, 26–29.
- [41]. Kokila, K.; Elavarasan, N.; Sujatha, V. *Diospyros montana* leaf extract-mediated synthesis of selenium nanoparticles and their biological applications. *New J. Chem.* **2017**, *41*, 7481–7490.
- [42]. Mosallam, F. M.; El-Sayyad, G. S.; Fathy, R. M.; El-Batal, A. I. Biomolecules-mediated synthesis of selenium nanoparticles using *Aspergillus oryzae* fermented Lupin extract and gamma radiation for hindering the growth of some multidrug-resistant bacteria and pathogenic fungi. *Microb. Pathog.* **2018**, *122*, 108–116.
- [43]. Sreekanth, T. V. M.; Pandurangan, M.; Kim, D. H.; Lee, Y. R. Green synthesis: In-vitro anticancer activity of silver nanoparticles on human cervical cancer cells. *J. Cluster Sci.* **2016**, *27*, 671–681.
- [44]. Ganapuram, B. R.; Alle, M.; Dadigala, R.; Dasari, A.; Maragoni, V.; Guttena, V. Catalytic reduction of methylene blue and Congo red dyes using green synthesized gold nanoparticles capped by *salmalia malabarica* gum. *Int. Nano Lett.* **2015**, *5*, 215–222.
- [45]. Rawat, V.; Sharma, A.; Bhatt, V. P.; Pratap Singh, R.; Maurya, I. K. Sunlight mediated green synthesis of silver nanoparticles using *Polygonatum graminifolium* leaf extract and their antibacterial activity. *Mater. Today* **2020**, *29*, 911–916.
- [46]. San Keskin, N. O.; Akbal Vural, O.; Abaci, S. Biosynthesis of noble selenium nanoparticles from *Lysinibacillus* sp. NOSK for antimicrobial, antibiofilm activity, and biocompatibility. *Geomicrobiol. J.* **2020**, *37*, 919–928.
- [47]. Boroumand, S.; Safari, M.; Shaabani, E.; Shirzad, M.; Faridi-Majidi, R. Selenium nanoparticles: synthesis, characterization and study of their cytotoxicity, antioxidant and antibacterial activity. *Mater. Res. Express* **2019**, *6*, 0850d8.
- [48]. Menon, S.; Agarwal, H.; Rajeshkumar, S.; Jacqueline Rosy, P.; Shanmugam, V. K. Investigating the antimicrobial activities of the biosynthesized selenium nanoparticles and its statistical analysis. *Bionanoscience* **2020**, *10*, 122–135.
- [49]. Shoeibi, S.; Mashreghi, M. Biosynthesis of selenium nanoparticles using *Enterococcus faecalis* and evaluation of their antibacterial activities. *J. Trace Elem. Med. Biol.* **2017**, *39*, 135–139.
- [50]. Shakibaie, M.; Salari Mohazab, N.; Ayatollahi Mousavi, S. A. Antifungal Activity of Selenium Nanoparticles Synthesized by *Bacillus* species Msh-1 Against *Aspergillus fumigatus* and *Candida albicans*. *Jundishapur J. Microbiol.* **2015**, *8*, e26381.
- [51]. Shahabadi, N.; Zendehehshem, S.; Khademi, F. Selenium nanoparticles: Synthesis, in-vitro cytotoxicity, antioxidant activity and interaction studies with ct-DNA and HSA, Hb and Cyt c serum proteins. *Biotechnol. Rep. (Amst.)* **2021**, *30*, e00615.
- [52]. Saha, J.; Begum, A.; Mukherjee, A.; Kumar, S. A novel green synthesis of silver nanoparticles and their catalytic action in reduction of Methylene Blue dye. *Sustain. Environ. Res.* **2017**, *27*, 245–250.
- [53]. Cittrarasu, V.; Kaliannan, D.; Dharman, K.; Maluventhen, V.; Easwaran, M.; Liu, W. C.; Balasubramanian, B.; Arumugam, M. Green synthesis of selenium nanoparticles mediated from *Ceropegia bulbosa* Roxb extract and its cytotoxicity, antimicrobial, mosquitocidal and photocatalytic activities. *Sci. Rep.* **2021**, *11*, 1032.



Copyright © 2023 by Authors. This work is published and licensed by Atlanta Publishing House LLC, Atlanta, GA, USA. The full terms of this license are available at <http://www.eurjchem.com/index.php/eurjchem/pages/view/terms> and incorporate the Creative Commons Attribution-Non Commercial (CC BY NC) (International, v4.0) License (<http://creativecommons.org/licenses/by-nc/4.0>). By accessing the work, you hereby accept the Terms. This is an open access article distributed under the terms and conditions of the CC BY NC License, which permits unrestricted non-commercial use, distribution, and reproduction in any medium, provided the original work is properly cited without any further permission from Atlanta Publishing House LLC (European Journal of Chemistry). No use, distribution, or reproduction is permitted which does not comply with these terms. Permissions for commercial use of this work beyond the scope of the License (<http://www.eurjchem.com/index.php/eurjchem/pages/view/terms>) are administered by Atlanta Publishing House LLC (European Journal of Chemistry).